

RESEARCH REPORT

MpWIP regulates air pore complex development in the liverwort *Marchantia polymorpha*

Victor A. S. Jones and Liam Dolan*

ABSTRACT

The colonisation of the land by plants was accompanied by the evolution of complex tissues and multicellular structures comprising different cell types as morphological adaptations to the terrestrial environment. Here, we show that the single WIP protein in the early-diverging land plant *Marchantia polymorpha* L. is required for the development of the multicellular gas exchange structure: the air pore complex. This 16-cell barrel-shaped structure surrounds an opening between epidermal cells that facilitates the exchange of gases between the chamber containing the photosynthetic cells inside the plant and the air outside. MpWIP is expressed in cells of the developing air pore complex and the morphogenesis of the complex is defective in plants with reduced MpWIP function. The role of WIP proteins in the control of different multicellular structures in *M. polymorpha* and the flowering plant *Arabidopsis thaliana* suggests that these proteins controlled the development of multicellular structures in the common ancestor of land plants. We hypothesise that WIP genes were subsequently co-opted in the control of morphogenesis of novel multicellular structures that evolved during the diversification of land plants.

KEY WORDS: *Marchantia polymorpha*, Air pore complex, WIP protein

INTRODUCTION

Morphological diversity increased dramatically after plants colonised the land some time before 460 million years ago (Kenrick and Crane, 1997). The evolution of unicellular and multicellular structures with specialised functions in the outermost cell layer – the epidermis – provided plants with the means to increase the surface area over which CO₂ uptake from the atmosphere occurred, and to extract water and inorganic nutrients from the early soil. Some specialised epidermal structures are present in all extant lineages of land plants. For example, tip-growing rhizoids and root hairs emerge from the epidermis to provide anchorage and to take up water and nutrients from the soil (Jones and Dolan, 2012). The phylogenetic distribution of others is more restricted; stomata, valves in the epidermis consisting of two specialised guard cells that open and close to regulate gas exchange, develop in all land plant lineages except the early diverging Marchantiophyta (liverworts). In one group of liverworts, the

Marchantiidae, the evolution of complex tissues has been accompanied by an independent evolution of a multicellular epidermal structure that facilitates gas exchange: the air pore complex (Crandall-Stotler et al., 2009). We report here that the zinc-finger protein MpWIP is necessary for the morphogenesis of the air pore complex in the epidermis of *Marchantia polymorpha*.

RESULTS AND DISCUSSION

A gain-of-function mutation in MpWIP causes defective development of the dorsal epidermis

To identify genetic mechanisms controlling the development of specialised morphological structures that operated in the earliest land plants, we screened for mutants with defects in the development of epidermal structures in the liverwort *Marchantia polymorpha*, a member of one of the earliest diverging groups of land plants. Multicellular air pore complexes, gemma cups and gemmae develop on the dorsal epidermis of *M. polymorpha* (Fig. 1A,C), while unicellular rhizoids and multicellular membranous outgrowths (scales) develop on the ventral epidermis (Fig. 1B,D). In a screen of T-DNA insertion mutants (Honkanen et al., 2016), we isolated a mutant, *vj7*, that develops rhizoids from the epidermal cells of the mature dorsal epidermis (3.76 rhizoids/mm², *n*=5); rhizoids do not develop on the dorsal epidermis of the wild type (Fig. 1E,F). We crossed this mutant to the wild-type Tak-1 to determine its inheritance; of 293 F1 plants scored, 131 expressed the mutant phenotype and 162 the wild-type phenotype (segregation ratio 1:1.24, χ^2 *P*=0.07), demonstrating that the dorsal rhizoid phenotype is controlled by a single Mendelian locus. We located a T-DNA insertion in this line and genotyped 106 of the above F1 offspring for its presence. Seventy-four F1s displayed the mutant phenotype and possessed the insertion, while the remaining 34 were wild type and lacked the insertion, indicating that this insertion is linked to the mutant phenotype. The insertion lies 764 bp upstream of the transcriptional start site of a gene encoding a member of the WIP zinc-finger protein family, MpWIP (GenBank: KX645870) (Figs 1G, S1, S2).

We hypothesised that the T-DNA insertion in *vj7* would impact the transcription of the MpWIP gene 3' from the T-DNA right border. To quantify the effects of this insertion on MpWIP expression, we measured the steady-state levels of MpWIP transcript in the wild-type and mutant *vj7*. MpWIP transcript levels were almost four times higher in *vj7* than in the wild-type Tak-2 (Fig. 1H), consistent with the hypothesis that *vj7* is a gain-of-function Mpwip mutant. To independently verify that MpWIP gain of function induces the development of rhizoids on the dorsal surface of *M. polymorpha*, we expressed MpWIP under the control of the constitutively active OsACTIN promoter (*pro*-OsACT: MpWIP) (Breuninger et al., 2016), and isolated a line in which the level of MpWIP transcript is twice that seen in the wild type (Fig. 1H). Plants of this line developed ectopic rhizoids on the dorsal surface, as observed in *vj7* but not the wild-type Tak-2 (Fig. 1I). This is

Department of Plant Sciences, University of Oxford, Oxford OX1 3RB, UK.

*Author for correspondence (liam.dolan@plants.ox.ac.uk)

 L.D., 0000-0003-1206-7096

This is an Open Access article distributed under the terms of the Creative Commons Attribution License (<http://creativecommons.org/licenses/by/3.0>), which permits unrestricted use, distribution and reproduction in any medium provided that the original work is properly attributed.

Received 11 September 2016; Accepted 26 January 2017

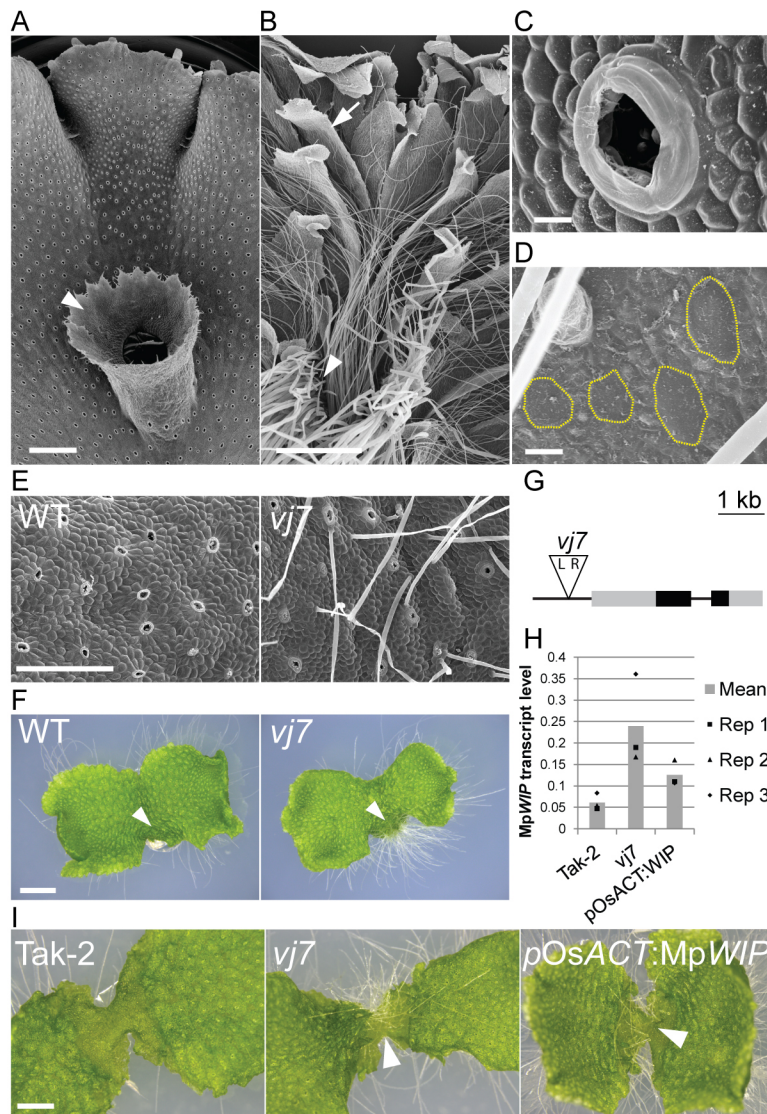


Fig. 1. A gain-of-function mutant of MpWIP develops ectopic rhizoids on the dorsal surface. (A) Air pores and gemma cups (arrowhead) are produced on the dorsal thallus surface. Scale bar: 1 mm, apex at the top. (B) Scales (arrow) and rhizoids (arrowhead) are produced on the ventral thallus surface. Scale bar: 1 mm, apex at the top. (C) Detail of air pore complex. Scale bar: 20 μ m. (D) Detail of ventral rhizoid patch. Cells that will develop into rhizoids (yellow outlines) are separated by non-rhizoid cells. Scale bar: 20 μ m. (E) Rhizoids develop on the dorsal surface of older parts of the mature thallus of *vj7* but not wild type at 43 days. Scale bar: 500 μ m. (F) Sporelings of *vj7* produce rhizoids on the oldest part of the dorsal thallus surface (arrowhead). This region of wild-type sporelings lacks rhizoids at 28 days. Scale bar: 2 mm. (G) The T-DNA insertion that co-segregates with the mutant phenotype in *vj7* is located 5' to *MpWIP*. Boxes represent exons: black, CDS, grey, untranslated regions. (H) *MpWIP* transcript levels are greater in mutant *vj7* and *proOsACT:MpWIP* than in wild-type Tak-2 in 14-day-old gemmalings. (I) Expression of *MpWIP* driven by the constitutive promoter *proOsACT* causes the development of ectopic rhizoids (arrowheads), as in mutant *vj7* in 10-day-old gemmalings. Scale bar: 1 mm.

consistent with the hypothesis that a gain of *MpWIP* function causes the development of ectopic rhizoids in mutant *vj7*. We conclude that *vj7* is a gain-of-function mutant of *MpWIP* and designated it *Mpwpip-1^{GOF}*.

The *MpWIP* promoter is active in developing air pores

To investigate where the *MpWIP* promoter is active in the wild type, we expressed *3xYFP-NLS* under the control of a 4.7 kb fragment of genomic DNA upstream of the coding DNA sequence (CDS) of

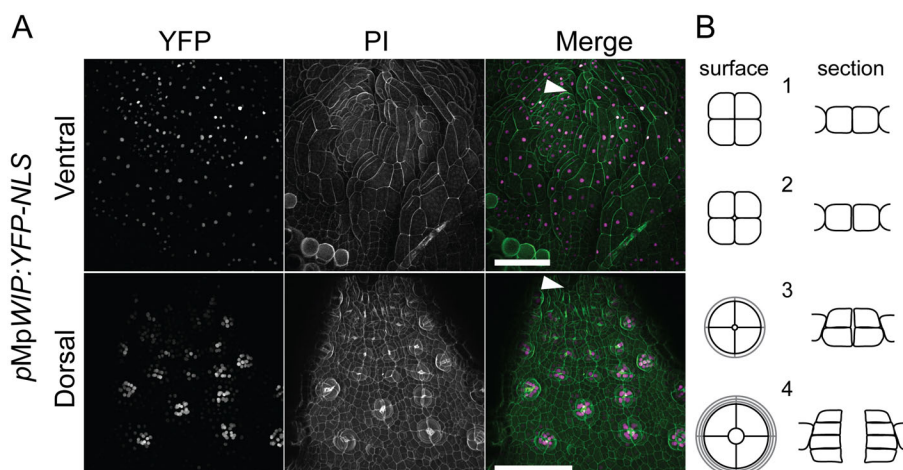


Fig. 2. The *MpWIP* promoter is active in the ventral apical region and in developing air pores. (A) Apical region of the ventral and dorsal surface of the thallus of a *proMpWIP:3xYFP-NLS* 9-day-old gemmaling. Scale bars: 100 μ m; arrowheads indicate the apex. (B) Schematic of the stages of air pore development. A schizogen opening develops at the point where four epidermal cells meet (stages 1 and 2). Periclinal divisions then give rise to a stack of rings, each consisting of four cells (stages 3 and 4). Surface view (left) and cross-section (right). Based on data from Apostolakis and Galatis (1985a).

MpWIP (*pro*MpWIP:YFP-NLS). In plants transformed with *pro*MpWIP:YFP-NLS, fluorescent protein was detected in cells in the apical region of both the ventral and dorsal sides of the thallus (Fig. 2A). The activity of the promoter in the ventral apical region, where rhizoids initiate, is consistent with a possible role for MpWIP in promoting rhizoid development. On the dorsal side of the thallus, the MpWIP promoter was most active in cells of developing air pore complexes (Fig. 2A), with lower activity in the surrounding epidermal cells. Air pores initiate as schizogenous openings that form in the epidermis at points where four cells meet (Apostolakis and Galatis, 1985a). The four cells surrounding each opening divide periclinally and differentiate to form the multiple tiers of the barrel-shaped air pore (Fig. 2B) (Apostolakis and Galatis, 1985a). Air chambers form below the air pores and consist of schizogenous intercellular cavities in which filaments of photosynthetic cells develop (Apostolakis and Galatis, 1985b; Ishizaki et al., 2013; Mirbel, 1835). Low levels of *pro*MpWIP activity were detected in all cells near the apex before air pore differentiation is visible, and this activity increased in the dividing cells of the developing air pore complex. The strong promoter activity in cells of the air pore complexes compared with surrounding cells is first apparent at the four-cell stage, when the cells surrounding the schizogenous opening first enlarge relative to the surrounding epidermal cells (Fig. 2A,B). Strong expression continues during the periclinal divisions that generate the tiered 16-cell air pore complex (Fig. 2A, B). The activity of the MpWIP promoter during the formation of air pore complexes suggested that MpWIP could be involved in their development.

MpWIP is required for air pore development

To determine whether MpWIP is required for rhizoid or air pore complex development, we generated plants with decreased MpWIP function. We expressed two different artificial microRNAs based on *MpmiR160* (Flores-Sandoval et al., 2016) that target either the 3' UTR (*amiR-MpWIP-3' UTR*^{MpmiR160}) or CDS (*amiR-MpWIP-CDS*^{MpmiR160}) of MpWIP under the control of *pro*OsACT. Steady-state levels of MpWIP transcript are reduced to approximately half wild-type levels in plants transformed with *pro*OsACT:*amiR-MpWIP-3' UTR*^{MpmiR160} or *pro*OsACT:*amiR-MpWIP-CDS*^{MpmiR160} (Fig. 3A,B). The formation of the air chambers is delayed or abolished in the MpWIP knockdown lines, and consequently the reticulated pattern of dark-green air chambers characteristic of the wild type is absent (Fig. 3A); this is in contrast to the *Mpwip-1_{GOF}* mutant, in which the density of air pore production is similar to the wild type (Fig. S3). Furthermore, the regular 16-cell structure of the wild-type air pore complex does not develop (Fig. 3C). Air pore development begins with the formation of schizogenous openings at the point where four cells meet, exactly as it does in the wild type (Fig. S4A). However, the periclinal divisions that form the tiers of the air pore complex in wild type mostly fail to occur in the knockdown lines. Instead, cells divide anticlinally, forming a single tier of more than four cells surrounding the pore (Fig. S4B). This indicates that reducing the level of MpWIP transcript disrupts air pore morphogenesis after the four-cell stage, consistent with a role for MpWIP in air pore complex and air chamber development suggested by the activity of *pro*MpWIP during air pore development (Fig. 2A). We were unable to quantify rhizoid density, but rhizoid development was indistinguishable from the wild type. Together, these data indicate that MpWIP activity is required for the differentiation of air pore complexes, but do not provide evidence that it is necessary for rhizoid development.

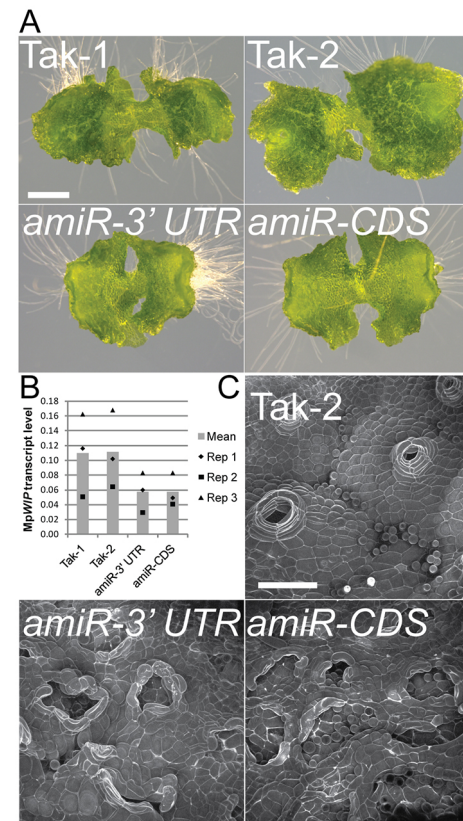


Fig. 3. Reduced MpWIP expression causes defects in air pore development. (A) The dark-green air chambers seen in the wild type (Tak-1, Tak-2) do not develop in plants transformed with *pro*OsACT:*amiR-MpWIP-3' UTR*^{MpmiR160} or *pro*OsACT:*amiR-MpWIP-CDS*^{MpmiR160}. Images taken in 10-day-old gemmings. Scale bar: 1 mm. (B) MpWIP transcript levels are reduced in lines transformed with *pro*OsACT:*amiR-MpWIP-3' UTR*^{MpmiR160} or *pro*OsACT:*amiR-MpWIP-CDS*^{MpmiR160}. Values are from 10-day-old gemmings. (C) Plants with reduced MpWIP transcript levels develop air pores with defective morphology, lacking the regular 16-cell air pore complex structure that develops in the wild type (Tak-2). CSLM: images are gemmings PI stained at 9 days. Scale bar: 100 μ m.

MpWIP may act as a transcriptional repressor

At least one WIP protein, AtNO TRANSMITTING TRACT (AtNTT), binds DNA (Marsch-Martínez et al., 2014). To determine whether MpWIP promotes rhizoid identity and air pore complex development through transcriptional activation or repression, we expressed chimeric dominant repressor and activator versions of MpWIP separately in transgenic plants. To generate the dominant repressor, we fused an SRDX repressive domain (Hiratsu et al., 2003) to the C-terminus of MpWIP; to make the dominant activator, we fused a VP16 activator domain to the C-terminus (Liu and Stewart, 2016; Sadowski et al., 1988; Wilde et al., 1994). Each of these fusion proteins was expressed using the constitutive CaMV 35S promoter (*pro*35S:MpWIP-SRDX and *pro*35S:MpWIP-VP16). If MpWIP promotes rhizoid and air pore differentiation via transcriptional repression, we predicted that: (1) supernumerary rhizoids would develop on plants that express MpWIP-SRDX, as observed in plants overexpressing MpWIP function (Fig. 1E,F,H,I); and (2) plants expressing MpWIP-VP16 would develop a defective air pore phenotype similar to that caused by a loss of MpWIP function in *pro*OsACT:*amiR-MpWIP-3' UTR*^{MpmiR160} and *pro*OsACT:*amiR-MpWIP-CDS*^{MpmiR160} lines (Fig. 3A-C).

Plants transformed with *pro*35S:MpWIP:SRDX that expressed the transgene (Fig. 4A) developed a dense growth of ectopic rhizoids on

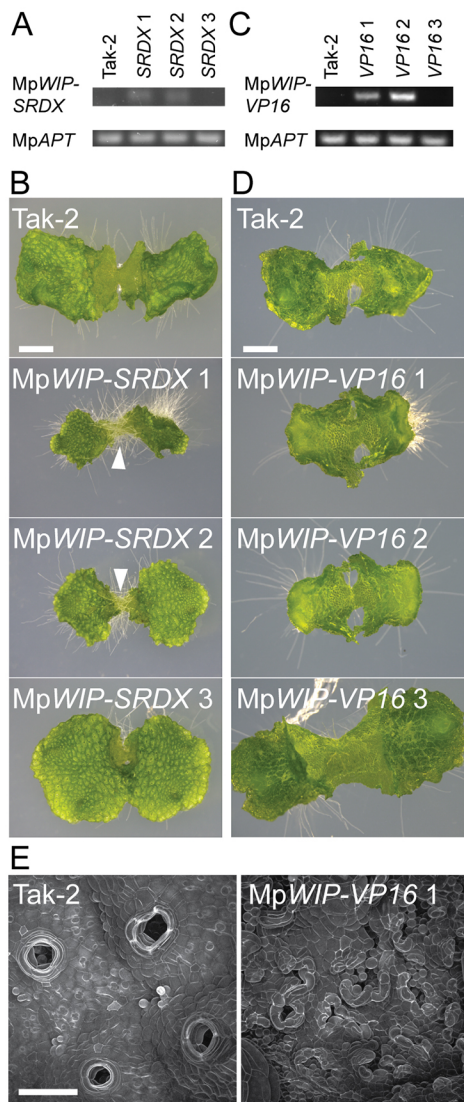


Fig. 4. Expression of the dominant repressor MpWIP-SRDX or the dominant activator MpWIP-VP16 causes the development of ectopic rhizoids or defective air pores, respectively. (A) MpWIP-SRDX transcript is detected in lines *pro35S:MpWIP:SRDX* 1 and 2 but not in *pro35S:MpWIP:SRDX* 3 or Tak-2. Samples are from 12-day-old gemmalings. (B) The lines that express MpWIP-SRDX (*pro35S:MpWIP:SRDX* 1 and 2) develop ectopic rhizoids on the dorsal surface (arrowheads). Images are of 12-day-old gemmalings. Scale bar: 2 mm. (C) MpWIP-VP16 transcript is detected in lines *pro35S:MpWIP:VP16* 1 and 2 but not *pro35S:MpWIP:VP16* 3 or Tak-2. Samples are from 10-day-old gemmalings. (D) Air chamber development is defective in lines that express MpWIP-VP16 (*pro35S:MpWIP:VP16* 1 and 2). Images are of 10-day-old gemmalings. Scale bar: 1 mm. (E) Air pore complex morphology is aberrant in lines that express MpWIP-VP16. CSLM: images are gemmalings PI stained at 10 days. Scale bar: 100 μ m.

the dorsal surface of the thallus, while air pore development was similar to wild type (Fig. 4C). This is similar to the phenotype of the *Mpwip*^{GOF} mutant and *proOsACT:MpWIP* line (Fig. 1E,F,I). The expression of a repressive form of MpWIP therefore results in the development of plants that are morphologically similar to plants that overexpress native MpWIP, consistent with the hypothesis that MpWIP is a transcriptional repressor. Plants that express the MpWIP-VP16 transgene (Fig. 4C) developed phenotypic defects comparable with those in lines with reduced MpWIP function, where air chamber (Figs 4D and 3A) and air pore complex

development are defective (Figs 4E and 3C). This suggests that expression of a form of MpWIP that promotes transcriptional activation has developmental effects similar to a loss of MpWIP function. Therefore, the phenotypes of both MpWIP:SRDX and MpWIP:VP16 lines are consistent with the hypothesis that MpWIP promotes the morphogenesis of air pore complexes through transcriptional repression.

We conclude that MpWIP is necessary for the morphogenesis of the multicellular air pore complex in the dorsal epidermis of *M. polymorpha*; air pore morphology is defective in plants with reduced WIP protein activity. WIP genes are also required for the development of various multicellular structures in the angiosperm *A. thaliana*. For example, AtNTT is a WIP protein required for the development of the replum, a structure that facilitates dehiscence and seed dispersal from *A. thaliana* fruits (Marsch-Martinez et al., 2014) – cell number is reduced in the repla of *Atnnt* mutant fruits compared with wild type. Roots do not form in *Atnnt Atwip4 Atwip5* triple mutants, demonstrating a requirement for these three related WIP proteins in the development of the distal stem cells of the root during embryogenesis (Crawford et al., 2015). Incomplete veins form in *Atdefectively organised tributaries5* (*Atdot5*) mutants, indicating the requirement of the WIP protein AtDOT5 in leaf vein development (Petricka et al., 2008). The demonstration that WIP proteins control the development of different multicellular structures in both early-diverging land plants and angiosperms (the latest-derived land plants) leads us to propose that WIP proteins control the development of multicellular structures in the common ancestor of *M. polymorpha* and *A. thaliana*, a close relative of the earliest land plants. We hypothesise that the subsequent duplication of WIP genes and neofunctionalisation of WIP proteins promoted the development of novel multicellular structures that evolved as the morphologies of land plants diversified.

MATERIALS AND METHODS

Plasmid construction

The generation of vectors for the constitutive expression of MpWIP, fusion proteins and artificial microRNAs, and of the MpWIP promoter reporter construct, is described in the supplementary Materials and Methods. See Table S1 for oligonucleotide sequences.

Phylogenetic analysis

MpWIP was aligned with WIP proteins from other land plants and the most similar non-WIP proteins from *M. polymorpha* and *A. thaliana*. This alignment was manually trimmed and used to infer a maximum-likelihood phylogeny. For further details, see the supplementary Materials and Methods.

Plant material and growth

Tak-1 male and Tak-2 female wild-type accessions (Ishizaki et al., 2008) were used in this study. Mutant *vj7* was isolated in a mutant screen of spores from a cross between Tak-1 and Tak-2 transformed with the T-DNA vector pCambia1300 (Honkanen et al., 2016). Plants were grown as previously described (Honkanen et al., 2016).

Microscopy

Images were obtained using a Leica M165FC stereomicroscope, Leica M series Plan APO 1.0 \times objective and Leica DFC310 FX camera. For confocal scanning laser microscopy (CSLM), plants were stained with 15 μ M propidium iodide for 15 min, then submerged in water. Images were acquired with a Leica SP5 confocal microscope using a Leica HCX APO 40 \times /0.80 W U-V-I dipping lens with sequential scans. YFP fluorescence was detected using excitation at 514 nm with an argon laser and emission was measured between 524 and 568 nm using an Acousto-Optic Tunable Filter. PI was excited at 543 nm using a helium-neon laser and emission

measured between 568 and 659 nm. Images were processed using FIJI to create brightest-point 3d projections (Schindelin et al., 2012).

For scanning electron microscopy, samples were fixed in dry methanol, critical point dried using a Tousimis Autosamdri-815, mounted on aluminium stubs and coated with a gold/palladium mixture using a Quorum Technologies SC7640 sputter coater. Samples were imaged immediately with a JEOL JSM-5510 SEM.

Molecular analysis of mutant *vj7* and gene expression analysis

Genomic sequences flanking T-DNA insertions were isolated by TAIL-PCR as previously described (Proust et al., 2016). Genes near the site of the insertion linked to the mutant phenotype in line *vj7* were identified using the blastn algorithm, with 5 kb of genomic sequence 3' and 5' to the insertion site as the template, to query an *M. polymorpha* transcriptome (Honkanen et al., 2016). RNA extraction, cDNA synthesis and quantitative PCRs (qPCRs) were carried out as previously described (Breuninger et al., 2016). *MpACT* and *MpAPT* were used as reference genes (Saint-Marcoux et al., 2015).

Acknowledgements

We are grateful to Alexander J. Hetherington, Clément Champion, Bruno Catarino, Anna Thamm, Dr Holger Breuninger, Dr Clémence Bonnot, and Dr Ana Milhinhos for discussions and comments on the manuscript.

Competing interests

The authors declare no competing or financial interests.

Author contributions

Conceptualization, L.D.; Methodology, V.A.S.J., L.D.; Investigation, V.A.S.J.; Writing – Original Draft, V.A.S.J., L.D.; Writing – Review and Editing, V.A.S.J., L.D.; Supervision, L.D.; Funding Acquisition, L.D.

Funding

This research was funded by a European Research Council Advanced Grant (project number 25028; EVO-500 to L.D.). V.A.S.J. was funded by a Newton Abraham Studentship from the University of Oxford. Deposited in PMC for immediate release.

Supplementary information

Supplementary information available online at <http://dev.biologists.org/lookup/doi/10.1242/dev.144287.supplemental>

References

- Apostolakis, P. and Galatis, B. (1985a). Studies on the development of the air pores and air chambers of *Marchantia paleacea*. IV. Cell plate arrangement in initial aperture cells. *Protoplasma* **128**, 136–146.
- Apostolakis, P. and Galatis, B. (1985b). Studies on the development of the air pores and air chambers of *Marchantia paleacea* III. Microtubule organization in preprophase-prophase initial aperture cells—formation of incomplete preprophase microtubule bands. *Protoplasma* **128**, 120–135.
- Breuninger, H., Thamm, A., Streubel, S., Sakayama, H., Nishiyama, T. and Dolan, L. (2016). Diversification of a bHLH transcription factor family led to the evolution of antagonistically acting genes controlling root hair growth. *Curr. Biol.* **26**, 1622–1628.
- Crandall-Stotler, B., Stotler, R. E. and Long, D. G. (2009). Phylogeny and classification of the Marchantiophyta. *Edinburgh J. Bot.* **66**, 155.
- Crawford, B. C. W., Sewell, J., Golembeski, G., Roshan, C., Long, J. A. and Yanofsky, M. F. (2015). Genetic control of distal stem cell fate within root and embryonic meristems. *Science* **347**, 655–659.
- Flores-Sandoval, E., Dierschke, T., Fisher, T. J. and Bowman, J. L. (2016). Efficient and inducible use of artificial microRNAs in *Marchantia polymorpha*. *Plant Cell Physiol.* **57**, 281–290.
- Hiratsu, K., Matsui, K., Koyama, T. and Ohme-Takagi, M. (2003). Dominant repression of target genes by chimeric repressors that include the EAR motif, a repression domain, in *Arabidopsis*. *Plant J.* **34**, 733–739.
- Honkanen, S., Jones, V. A. S., Morieri, G., Champion, C., Hetherington, A. J., Kelly, S., Proust, H., Saint-Marcoux, D., Prescott, H. and Dolan, L. (2016). The mechanism forming the cell surface of tip-growing rooting cells is conserved among land plants. *Curr. Biol.* **26**, 3238–3244.
- Ishizaki, K., Chiyoda, S., Yamato, K. T. and Kohchi, T. (2008). Agrobacterium-mediated transformation of the haploid liverwort *Marchantia polymorpha* L., an emerging model for plant biology. *Plant Cell Physiol.* **49**, 1084–1091.
- Ishizaki, K., Mizutani, M., Shimamura, M., Masuda, A., Nishihama, R. and Kohchi, T. (2013). Essential role of the E3 ubiquitin ligase NOPPERABO1 in schizogenous intercellular space formation in the liverwort *Marchantia polymorpha*. *Plant Cell* **25**, 4075–4084.
- Jones, V. A. S. and Dolan, L. (2012). The evolution of root hairs and rhizoids. *Ann. Bot.* **110**, 205–212.
- Kenrick, P. R. and Crane, P. R. (1997). *The Origin and Early Diversification of Land Plants: A Cladistic Study*, 1st edn. Washington, DC: Smithsonian Institution Press.
- Liu, W. and Stewart, C. N. (2016). Plant synthetic promoters and transcription factors. *Curr. Opin. Biotechnol.* **37**, 36–44.
- Marsch-Martínez, N., Zúñiga-Mayo, V. M., Herrera-Ubaldo, H., Ouwerkerk, P. B., Pablo-Villa, J., Lozano-Sotomayor, P., Greco, R., Ballester, P., Balanzá, V., Kuijt, S. J. et al. (2014). The NTT transcription factor promotes replum development in *Arabidopsis* fruits. *Plant J.* **80**, 69–81.
- Mirbel, M. (1835). Recherches anatomiques et physiologiques sur le *Marchantia polymorpha*, pour servir à l'histoire du tissu cellulaire, de l'épiderme et des stomates. *Mém. l'Acad. R. des Sci. l'Inst. Fr.* **Tome XIII**, 337–373.
- Petricka, J. J., Clay, N. K. and Nelson, T. M. (2008). Vein patterning screens and the defectively organized tributaries mutants in *Arabidopsis thaliana*. *Plant J.* **56**, 251–263.
- Proust, H., Honkanen, S., Jones, V. A. S., Morieri, G., Prescott, H., Kelly, S., Ishizaki, K., Kohchi, T. and Dolan, L. (2016). RSL class I genes controlled the development of epidermal structures in the common ancestor of land plants. *Curr. Biol.* **26**, 93–99.
- Sadowski, I., Ma, J., Triezenberg, S. and Ptashne, M. (1988). GAL4-VP16 is an unusually potent transcriptional activator. *Nature* **335**, 563–564.
- Saint-Marcoux, D., Proust, H., Dolan, L. and Langdale, J. A. (2015). Identification of reference genes for real-time quantitative PCR experiments in the liverwort *Marchantia polymorpha*. *PLoS ONE* **10**, e0118678.
- Schindelin, J., Arganda-Carreras, I., Frise, E., Kaynig, V., Longair, M., Pietzsch, T., Preibisch, S., Rueden, C., Saalfeld, S., Schmid, B. et al. (2012). Fiji: an open-source platform for biological-image analysis. *Nat. Methods* **9**, 676–682.
- Wilde, R. J., Cooke, S. E., Brammar, W. J. and Schuch, W. (1994). Control of gene expression in plant cells using a 434:VP16 chimeric protein. *Plant Mol. Biol.* **24**, 381–388.